

Measurement of the D^{*-} polarization in the decay $B^0 \rightarrow D^{*-} \tau^+ \nu_\tau$

- A. Abdesselam,¹⁰³ I. Adachi,^{22, 18} K. Adamczyk,⁷⁷ J. K. Ahn,⁵⁰ H. Aihara,¹¹¹
S. Al Said,^{103, 47} K. Arinstein,^{5, 81} Y. Arita,⁶⁹ D. M. Asner,⁴ H. Atmacan,⁹⁹
V. Aulchenko,^{5, 81} T. Aushev,⁶⁸ R. Ayad,¹⁰³ T. Aziz,¹⁰⁴ V. Babu,¹⁰⁴ I. Badhrees,^{103, 46}
S. Bahinipati,²⁹ A. M. Bakich,¹⁰² Y. Ban,⁸⁶ V. Bansal,⁸⁴ E. Barberio,⁶⁴ M. Barrett,¹¹⁷
W. Bartel,¹⁰ P. Behera,³² C. Beleno,¹⁷ K. Belous,³⁶ M. Berger,¹⁰⁰ F. Bernlochner,³
D. Besson,⁶⁷ V. Bhardwaj,²⁸ B. Bhuyan,³⁰ T. Bilka,⁶ J. Biswal,⁴¹ T. Bloomfield,⁶⁴
A. Bobrov,^{5, 81} A. Bondar,^{5, 81} G. Bonvicini,¹¹⁷ A. Bozek,⁷⁷ M. Bračko,^{62, 41} N. Braun,⁴³
F. Breibek,³⁵ T. E. Browder,²¹ M. Campajola,^{38, 71} L. Cao,⁴³ G. Caria,⁶⁴ D. Červenkov,⁶
M.-C. Chang,¹³ P. Chang,⁷⁶ Y. Chao,⁷⁶ R. Cheaib,⁶⁵ V. Chekelian,⁶³ A. Chen,⁷⁴
K.-F. Chen,⁷⁶ B. G. Cheon,²⁰ K. Chilikin,⁵⁵ R. Chistov,^{55, 67} H. E. Cho,²⁰ K. Cho,⁴⁹
V. Chobanova,⁶³ S.-K. Choi,¹⁹ Y. Choi,¹⁰¹ S. Choudhury,³¹ D. Cinabro,¹¹⁷ J. Crnkovic,²⁷
S. Cunliffe,¹⁰ T. Czank,¹⁰⁹ M. Danilov,^{67, 55} N. Dash,²⁹ S. Di Carlo,⁵³ J. Dingfelder,³
Z. Doležal,⁶ T. V. Dong,^{22, 18} D. Dossett,⁶⁴ Z. Drásal,⁶ A. Drutskoy,^{55, 67} S. Dubey,²¹
D. Dutta,¹⁰⁴ S. Eidelman,^{5, 81} D. Epifanov,^{5, 81} J. E. Fast,⁸⁴ M. Feindt,⁴³ T. Ferber,¹⁰
A. Frey,¹⁷ O. Frost,¹⁰ B. G. Fulsom,⁸⁴ R. Garg,⁸⁵ V. Gaur,¹⁰⁴ N. Gabyshev,^{5, 81}
A. Garmash,^{5, 81} M. Gelb,⁴³ J. Gemmler,⁴³ D. Getzkow,¹⁵ F. Giordano,²⁷ A. Giri,³¹
P. Goldenzweig,⁴³ B. Golob,^{57, 41} D. Greenwald,¹⁰⁶ M. Grosse Perdekamp,^{27, 92} J. Grygier,⁴³
O. Grzymkowska,⁷⁷ Y. Guan,⁹ E. Guido,³⁹ H. Guo,⁹⁴ J. Haba,^{22, 18} P. Hamer,¹⁷ K. Hara,²²
T. Hara,^{22, 18} Y. Hasegawa,⁹⁶ J. Hasenbusch,³ K. Hayasaka,⁷⁹ H. Hayashii,⁷³ X. H. He,⁸⁶
M. Heck,⁴³ M. T. Hedges,²¹ D. Heffernan,⁸³ M. Heider,⁴³ A. Heller,⁴³ T. Higuchi,⁴⁴
S. Hirose,⁶⁹ T. Horiguchi,¹⁰⁹ Y. Hoshi,¹⁰⁸ K. Hoshina,¹¹⁴ W.-S. Hou,⁷⁶ Y. B. Hsiung,⁷⁶
C.-L. Hsu,¹⁰² K. Huang,⁷⁶ M. Huschle,⁴³ Y. Igarashi,²² T. Iijima,^{70, 69} M. Imamura,⁶⁹
K. Inami,⁶⁹ G. Inguglia,¹⁰ A. Ishikawa,¹⁰⁹ K. Itagaki,¹⁰⁹ R. Itoh,^{22, 18} M. Iwasaki,⁸²
Y. Iwasaki,²² S. Iwata,¹¹³ W. W. Jacobs,³³ I. Jaegle,¹² H. B. Jeon,⁵² S. Jia,² Y. Jin,¹¹¹
D. Joffe,⁴⁵ M. Jones,²¹ C. W. Joo,⁴⁴ K. K. Joo,⁸ T. Julius,⁶⁴ J. Kahn,⁵⁸ H. Kakuno,¹¹³
A. B. Kaliyar,³² J. H. Kang,¹¹⁹ K. H. Kang,⁵² P. Kapusta,⁷⁷ G. Karyan,¹⁰ S. U. Kataoka,⁷²
E. Kato,¹⁰⁹ Y. Kato,⁶⁹ P. Katrenko,^{68, 55} H. Kawai,⁷ T. Kawasaki,⁴⁸ T. Keck,⁴³ H. Kichimi,²²
C. Kiesling,⁶³ B. H. Kim,⁹⁵ C. H. Kim,²⁰ D. Y. Kim,⁹⁸ H. J. Kim,⁵² H.-J. Kim,¹¹⁹
J. B. Kim,⁵⁰ K. T. Kim,⁵⁰ S. H. Kim,²⁰ S. K. Kim,⁹⁵ Y. J. Kim,⁵⁰ T. Kimmel,¹¹⁶
H. Kindo,^{22, 18} K. Kinoshita,⁹ C. Kleinwort,¹⁰ J. Klucar,⁴¹ N. Kobayashi,¹¹² P. Kodyš,⁶
Y. Koga,⁶⁹ T. Konno,⁴⁸ S. Korpar,^{62, 41} D. Kotchetkov,²¹ R. T. Kouzes,⁸⁴ P. Križan,^{57, 41}
R. Kroeger,⁶⁵ J.-F. Krohn,⁶⁴ P. Krokovny,^{5, 81} B. Kronenbitter,⁴³ T. Kuhr,⁵⁸ R. Kulasiri,⁴⁵
R. Kumar,⁸⁸ T. Kumita,¹¹³ E. Kurihara,⁷ Y. Kuroki,⁸³ A. Kuzmin,^{5, 81} P. Kvasnička,⁶
Y.-J. Kwon,¹¹⁹ Y.-T. Lai,²² K. Lalwani,⁶⁰ J. S. Lange,¹⁵ I. S. Lee,²⁰ J. K. Lee,⁹⁵ J. Y. Lee,⁹⁵
S. C. Lee,⁵² M. Leitgab,^{27, 92} R. Leitner,⁶ D. Levit,¹⁰⁶ P. Lewis,²¹ C. H. Li,⁵⁶ H. Li,³³
L. K. Li,³⁴ Y. Li,¹¹⁶ Y. B. Li,⁸⁶ L. Li Gioi,⁶³ J. Libby,³² K. Lieret,⁵⁸ A. Limosani,⁶⁴
Z. Liptak,²¹ C. Liu,⁹⁴ Y. Liu,⁹ D. Liventsev,^{116, 22} A. Loos,⁹⁹ R. Louvot,⁵⁴ P.-C. Lu,⁷⁶
M. Lubej,⁴¹ T. Luo,¹⁴ J. MacNaughton,⁶⁶ M. Masuda,¹¹⁰ T. Matsuda,⁶⁶ D. Matvienko,^{5, 81}
J. T. McNeil,¹² M. Merola,^{38, 71} F. Metzner,⁴³ Y. Mikami,¹⁰⁹ K. Miyabayashi,⁷³
Y. Miyachi,¹¹⁸ H. Miyake,^{22, 18} H. Miyata,⁷⁹ Y. Miyazaki,⁶⁹ R. Mizuk,^{55, 67, 68}

G. B. Mohanty,¹⁰⁴ S. Mohanty,^{104, 115} H. K. Moon,⁵⁰ T. J. Moon,⁹⁵ T. Mori,⁶⁹ T. Morii,⁴⁴
 H.-G. Moser,⁶³ M. Mrvar,⁴¹ T. Müller,⁴³ N. Muramatsu,⁸⁹ R. Mussa,³⁹ Y. Nagasaka,²⁵
 Y. Nakahama,¹¹¹ I. Nakamura,^{22, 18} K. R. Nakamura,²² E. Nakano,⁸² H. Nakano,¹⁰⁹
 T. Nakano,⁹⁰ M. Nakao,^{22, 18} H. Nakayama,^{22, 18} H. Nakazawa,⁷⁶ T. Nanut,⁴¹ K. J. Nath,³⁰
 Z. Natkaniec,⁷⁷ M. Nayak,^{117, 22} K. Neichi,¹⁰⁸ C. Ng,¹¹¹ C. Niebuhr,¹⁰ M. Niyyama,⁵¹
 N. K. Nisar,⁸⁷ S. Nishida,^{22, 18} K. Nishimura,²¹ O. Nitoh,¹¹⁴ A. Ogawa,⁹² K. Ogawa,⁷⁹
 S. Ogawa,¹⁰⁷ T. Ohshima,⁶⁹ S. Okuno,⁴² S. L. Olsen,¹⁹ H. Ono,^{78, 79} Y. Ono,¹⁰⁹ Y. Onuki,¹¹¹
 W. Ostrowicz,⁷⁷ C. Oswald,³ H. Ozaki,^{22, 18} P. Pakhlov,^{55, 67} G. Pakhlova,^{55, 68} B. Pal,⁴
 E. Panzenböck,^{17, 73} S. Pardi,³⁸ C.-S. Park,¹¹⁹ C. W. Park,¹⁰¹ H. Park,⁵² K. S. Park,¹⁰¹
 S.-H. Park,¹¹⁹ S. Patra,²⁸ S. Paul,¹⁰⁶ I. Pavelkin,⁶⁸ T. K. Pedlar,⁵⁹ T. Peng,⁹⁴ L. Pesáñez,³
 R. Pestotnik,⁴¹ M. Peters,²¹ L. E. Piilonen,¹¹⁶ V. Popov,^{55, 68} K. Prasanth,¹⁰⁴ E. Prencipe,²⁴
 M. Prim,⁴³ K. Prothmann,^{63, 105} M. V. Purohit,⁹⁹ A. Rabusov,¹⁰⁶ J. Rauch,¹⁰⁶ B. Reisert,⁶³
 P. K. Resmi,³² E. Ribežl,⁴¹ M. Ritter,⁵⁸ J. Rorie,²¹ A. Rostomyan,¹⁰ M. Rozanska,⁷⁷
 S. Rummel,⁵⁸ G. Russo,³⁸ D. Sahoo,¹⁰⁴ H. Sahoo,⁶⁵ T. Saito,¹⁰⁹ Y. Sakai,^{22, 18}
 M. Salehi,^{61, 58} S. Sandilya,⁹ D. Santel,⁹ L. Santelj,²² T. Sanuki,¹⁰⁹ J. Sasaki,¹¹¹
 N. Sasao,⁵¹ Y. Sato,⁶⁹ V. Savinov,⁸⁷ T. Schlüter,⁵⁸ O. Schneider,⁵⁴ G. Schnell,^{1, 26}
 P. Schönmeier,¹⁰⁹ M. Schram,⁸⁴ J. Schueler,²¹ C. Schwanda,³⁵ A. J. Schwartz,⁹
 B. Schwenker,¹⁷ R. Seidl,⁹² Y. Seino,⁷⁹ D. Semmler,¹⁵ K. Senyo,¹¹⁸ O. Seon,⁶⁹ I. S. Seong,²¹
 M. E. Sevior,⁶⁴ L. Shang,³⁴ M. Shapkin,³⁶ V. Shebalin,²¹ C. P. Shen,² T.-A. Shibata,¹¹²
 H. Shibuya,¹⁰⁷ S. Shinomiya,⁸³ J.-G. Shiu,⁷⁶ B. Shwartz,^{5, 81} A. Sibidanov,¹⁰² F. Simon,⁶³
 J. B. Singh,⁸⁵ R. Sinha,³⁷ K. Smith,⁶⁴ A. Sokolov,³⁶ Y. Soloviev,¹⁰ E. Solovieva,⁵⁵
 S. Stanič,⁸⁰ M. Starič,⁴¹ M. Steder,¹⁰ Z. Stottler,¹¹⁶ J. F. Strube,⁸⁴ J. Stypula,⁷⁷
 S. Sugihara,¹¹¹ A. Sugiyama,⁹³ M. Sumihama,¹⁶ K. Sumisawa,^{22, 18} T. Sumiyoshi,¹¹³
 W. Sutcliffe,⁴³ K. Suzuki,⁶⁹ K. Suzuki,¹⁰⁰ S. Suzuki,⁹³ S. Y. Suzuki,²² Z. Suzuki,¹⁰⁹
 H. Takeichi,⁶⁹ M. Takizawa,^{97, 23, 91} U. Tamponi,³⁹ M. Tanaka,^{22, 18} S. Tanaka,^{22, 18}
 K. Tanida,⁴⁰ N. Taniguchi,²² Y. Tao,¹² G. N. Taylor,⁶⁴ F. Tenchini,¹⁰ Y. Teramoto,⁸²
 K. Trabelsi,⁵³ T. Tsuboyama,^{22, 18} M. Uchida,¹¹² T. Uchida,²² I. Ueda,²² S. Uehara,^{22, 18}
 T. Uglov,^{55, 68} Y. Unno,²⁰ S. Uno,^{22, 18} P. Urquijo,⁶⁴ Y. Ushiroda,^{22, 18} Y. Usov,^{5, 81}
 S. E. Vahsen,²¹ C. Van Hulse,¹ R. Van Tonder,⁴³ P. Vanhoefer,⁶³ G. Varner,²¹
 K. E. Varvell,¹⁰² K. Vervink,⁵⁴ A. Vinokurova,^{5, 81} V. Vorobyev,^{5, 81} A. Vossen,¹¹
 M. N. Wagner,¹⁵ E. Waheed,⁶⁴ B. Wang,⁶³ C. H. Wang,⁷⁵ M.-Z. Wang,⁷⁶ P. Wang,³⁴
 X. L. Wang,¹⁴ M. Watanabe,⁷⁹ Y. Watanabe,⁴² S. Watanuki,¹⁰⁹ R. Wedd,⁶⁴ S. Wehle,¹⁰
 E. Widmann,¹⁰⁰ J. Wiechczynski,⁷⁷ K. M. Williams,¹¹⁶ E. Won,⁵⁰ B. D. Yabsley,¹⁰²
 S. Yamada,²² H. Yamamoto,¹⁰⁹ Y. Yamashita,⁷⁸ S. B. Yang,⁵⁰ S. Yashchenko,¹⁰ H. Ye,¹⁰
 J. Yelton,¹² J. H. Yin,³⁴ Y. Yook,¹¹⁹ C. Z. Yuan,³⁴ Y. Yusa,⁷⁹ S. Zakharov,^{55, 68}
 C. C. Zhang,³⁴ J. Zhang,³⁴ L. M. Zhang,⁹⁴ Z. P. Zhang,⁹⁴ L. Zhao,⁹⁴ V. Zhilich,^{5, 81}
 V. Zhukova,^{55, 67} V. Zhulanov,^{5, 81} T. Zivko,⁴¹ A. Zupanc,^{57, 41} and N. Zwahlen⁵⁴

(The Belle Collaboration)

¹ University of the Basque Country UPV/EHU, 48080 Bilbao

² Beihang University, Beijing 100191

³ University of Bonn, 53115 Bonn

⁴ Brookhaven National Laboratory, Upton, New York 11973

⁵ Budker Institute of Nuclear Physics SB RAS, Novosibirsk 630090

⁶ Faculty of Mathematics and Physics, Charles University, 121 16 Prague

- ⁷*Chiba University, Chiba 263-8522*
- ⁸*Chonnam National University, Kwangju 660-701*
- ⁹*University of Cincinnati, Cincinnati, Ohio 45221*
- ¹⁰*Deutsches Elektronen-Synchrotron, 22607 Hamburg*
- ¹¹*Duke University, Durham, North Carolina 27708*
- ¹²*University of Florida, Gainesville, Florida 32611*
- ¹³*Department of Physics, Fu Jen Catholic University, Taipei 24205*
- ¹⁴*Key Laboratory of Nuclear Physics and Ion-beam Application (MOE) and Institute of Modern Physics, Fudan University, Shanghai 200443*
- ¹⁵*Justus-Liebig-Universität Gießen, 35392 Gießen*
- ¹⁶*Gifu University, Gifu 501-1193*
- ¹⁷*II. Physikalisches Institut, Georg-August-Universität Göttingen, 37073 Göttingen*
- ¹⁸*SOKENDAI (The Graduate University for Advanced Studies), Hayama 240-0193*
- ¹⁹*Gyeongsang National University, Chinju 660-701*
- ²⁰*Hanyang University, Seoul 133-791*
- ²¹*University of Hawaii, Honolulu, Hawaii 96822*
- ²²*High Energy Accelerator Research Organization (KEK), Tsukuba 305-0801*
- ²³*J-PARC Branch, KEK Theory Center, High Energy Accelerator Research Organization (KEK), Tsukuba 305-0801*
- ²⁴*Forschungszentrum Jülich, 52425 Jülich*
- ²⁵*Hiroshima Institute of Technology, Hiroshima 731-5193*
- ²⁶*IKERBASQUE, Basque Foundation for Science, 48013 Bilbao*
- ²⁷*University of Illinois at Urbana-Champaign, Urbana, Illinois 61801*
- ²⁸*Indian Institute of Science Education and Research Mohali, SAS Nagar, 140306*
- ²⁹*Indian Institute of Technology Bhubaneswar, Satya Nagar 751007*
- ³⁰*Indian Institute of Technology Guwahati, Assam 781039*
- ³¹*Indian Institute of Technology Hyderabad, Telangana 502285*
- ³²*Indian Institute of Technology Madras, Chennai 600036*
- ³³*Indiana University, Bloomington, Indiana 47408*
- ³⁴*Institute of High Energy Physics, Chinese Academy of Sciences, Beijing 100049*
- ³⁵*Institute of High Energy Physics, Vienna 1050*
- ³⁶*Institute for High Energy Physics, Protvino 142281*
- ³⁷*Institute of Mathematical Sciences, Chennai 600113*
- ³⁸*INFN - Sezione di Napoli, 80126 Napoli*
- ³⁹*INFN - Sezione di Torino, 10125 Torino*
- ⁴⁰*Advanced Science Research Center, Japan Atomic Energy Agency, Naka 319-1195*
- ⁴¹*J. Stefan Institute, 1000 Ljubljana*
- ⁴²*Kanagawa University, Yokohama 221-8686*
- ⁴³*Institut für Experimentelle Teilchenphysik, Karlsruher Institut für Technologie, 76131 Karlsruhe*
- ⁴⁴*Kavli Institute for the Physics and Mathematics of the Universe (WPI), University of Tokyo, Kashiwa 277-8583*
- ⁴⁵*Kennesaw State University, Kennesaw, Georgia 30144*
- ⁴⁶*King Abdulaziz City for Science and Technology, Riyadh 11442*

- ⁴⁷*Department of Physics, Faculty of Science,
King Abdulaziz University, Jeddah 21589*
- ⁴⁸*Kitasato University, Sagamihara 252-0373*
- ⁴⁹*Korea Institute of Science and Technology Information, Daejeon 305-806*
- ⁵⁰*Korea University, Seoul 136-713*
- ⁵¹*Kyoto University, Kyoto 606-8502*
- ⁵²*Kyungpook National University, Daegu 702-701*
- ⁵³*LAL, Univ. Paris-Sud, CNRS/IN2P3, Université Paris-Saclay, Orsay*
- ⁵⁴*École Polytechnique Fédérale de Lausanne (EPFL), Lausanne 1015*
- ⁵⁵*P.N. Lebedev Physical Institute of the Russian Academy of Sciences, Moscow 119991*
- ⁵⁶*Liaoning Normal University, Dalian 116029*
- ⁵⁷*Faculty of Mathematics and Physics,
University of Ljubljana, 1000 Ljubljana*
- ⁵⁸*Ludwig Maximilians University, 80539 Munich*
- ⁵⁹*Luther College, Decorah, Iowa 52101*
- ⁶⁰*Malaviya National Institute of Technology Jaipur, Jaipur 302017*
- ⁶¹*University of Malaya, 50603 Kuala Lumpur*
- ⁶²*University of Maribor, 2000 Maribor*
- ⁶³*Max-Planck-Institut für Physik, 80805 München*
- ⁶⁴*School of Physics, University of Melbourne, Victoria 3010*
- ⁶⁵*University of Mississippi, University, Mississippi 38677*
- ⁶⁶*University of Miyazaki, Miyazaki 889-2192*
- ⁶⁷*Moscow Physical Engineering Institute, Moscow 115409*
- ⁶⁸*Moscow Institute of Physics and Technology, Moscow Region 141700*
- ⁶⁹*Graduate School of Science, Nagoya University, Nagoya 464-8602*
- ⁷⁰*Kobayashi-Maskawa Institute, Nagoya University, Nagoya 464-8602*
- ⁷¹*Università di Napoli Federico II, 80055 Napoli*
- ⁷²*Nara University of Education, Nara 630-8528*
- ⁷³*Nara Women's University, Nara 630-8506*
- ⁷⁴*National Central University, Chung-li 32054*
- ⁷⁵*National United University, Miao Li 36003*
- ⁷⁶*Department of Physics, National Taiwan University, Taipei 10617*
- ⁷⁷*H. Niewodniczanski Institute of Nuclear Physics, Krakow 31-342*
- ⁷⁸*Nippon Dental University, Niigata 951-8580*
- ⁷⁹*Niigata University, Niigata 950-2181*
- ⁸⁰*University of Nova Gorica, 5000 Nova Gorica*
- ⁸¹*Novosibirsk State University, Novosibirsk 630090*
- ⁸²*Osaka City University, Osaka 558-8585*
- ⁸³*Osaka University, Osaka 565-0871*
- ⁸⁴*Pacific Northwest National Laboratory, Richland, Washington 99352*
- ⁸⁵*Panjab University, Chandigarh 160014*
- ⁸⁶*Peking University, Beijing 100871*
- ⁸⁷*University of Pittsburgh, Pittsburgh, Pennsylvania 15260*
- ⁸⁸*Punjab Agricultural University, Ludhiana 141004*
- ⁸⁹*Research Center for Electron Photon Science,
Tohoku University, Sendai 980-8578*
- ⁹⁰*Research Center for Nuclear Physics, Osaka University, Osaka 567-0047*

⁹¹ *Theoretical Research Division, Nishina Center, RIKEN, Saitama 351-0198*

⁹² *RIKEN BNL Research Center, Upton, New York 11973*

⁹³ *Saga University, Saga 840-8502*

⁹⁴ *University of Science and Technology of China, Hefei 230026*

⁹⁵ *Seoul National University, Seoul 151-742*

⁹⁶ *Shinshu University, Nagano 390-8621*

⁹⁷ *Showa Pharmaceutical University, Tokyo 194-8543*

⁹⁸ *Soongsil University, Seoul 156-743*

⁹⁹ *University of South Carolina, Columbia, South Carolina 29208*

¹⁰⁰ *Stefan Meyer Institute for Subatomic Physics, Vienna 1090*

¹⁰¹ *Sungkyunkwan University, Suwon 440-746*

¹⁰² *School of Physics, University of Sydney, New South Wales 2006*

¹⁰³ *Department of Physics, Faculty of Science, University of Tabuk, Tabuk 71451*

¹⁰⁴ *Tata Institute of Fundamental Research, Mumbai 400005*

¹⁰⁵ *Excellence Cluster Universe, Technische Universität München, 85748 Garching*

¹⁰⁶ *Department of Physics, Technische Universität München, 85748 Garching*

¹⁰⁷ *Toho University, Funabashi 274-8510*

¹⁰⁸ *Tohoku Gakuin University, Tagajo 985-8537*

¹⁰⁹ *Department of Physics, Tohoku University, Sendai 980-8578*

¹¹⁰ *Earthquake Research Institute, University of Tokyo, Tokyo 113-0032*

¹¹¹ *Department of Physics, University of Tokyo, Tokyo 113-0033*

¹¹² *Tokyo Institute of Technology, Tokyo 152-8550*

¹¹³ *Tokyo Metropolitan University, Tokyo 192-0397*

¹¹⁴ *Tokyo University of Agriculture and Technology, Tokyo 184-8588*

¹¹⁵ *Utkal University, Bhubaneswar 751004*

¹¹⁶ *Virginia Polytechnic Institute and State University, Blacksburg, Virginia 24061*

¹¹⁷ *Wayne State University, Detroit, Michigan 48202*

¹¹⁸ *Yamagata University, Yamagata 990-8560*

¹¹⁹ *Yonsei University, Seoul 120-749*

Abstract

We report the first measurement of the D^{*-} meson polarization in the decay $B^0 \rightarrow D^{*-} \tau^+ \nu_\tau$ using the full data sample of 772×10^6 $B\bar{B}$ pairs recorded with the Belle detector at the KEKB electron-positron collider. Our result, $F_L^{D^*} = 0.60 \pm 0.08(\text{stat}) \pm 0.04(\text{sys})$, where $F_L^{D^*}$ denotes the D^{*-} meson longitudinal polarization fraction, agrees within about 1.7 standard deviations of the standard model prediction.

INTRODUCTION

Decays of B mesons to final states containing τ leptons provide an important test-bed for the standard model (SM) and its extensions. Of special interest are theoretically well-controlled semitauonic decays $B \rightarrow \bar{D}^{(*)}\tau^+\nu_\tau$ [1], where new physics (NP) may contribute at tree level. Complementary sensitivities of the decays $B \rightarrow \bar{D}\tau^+\nu_\tau$ and $B \rightarrow \bar{D}^*\tau^+\nu_\tau$ to various SM extensions, and the rich spectrum of kinematical observables accessible in the three-body final states, enable comprehensive studies of the underlying dynamics in $\bar{b} \rightarrow \bar{c}\tau^+\nu_\tau$ transitions [2, 3]. This potential is still far from being fully explored, primarily due to the inherent measurement challenges associated with multiple neutrino final states.

The decays $B \rightarrow \bar{D}^{(*)}\tau^+\nu_\tau$ have been studied experimentally by Belle [4–8], BaBar [9, 10], and LHCb [11, 12]. So far, the experiments measured the branching fractions $\mathcal{B}(B \rightarrow \bar{D}^{(*)}\tau^+\nu_\tau)$, or the ratios $R(D^{(*)}) = \mathcal{B}(B \rightarrow \bar{D}^{(*)}\tau^+\nu_\tau)/\mathcal{B}(B \rightarrow \bar{D}^{(*)}\ell^+\nu_\ell)$, ($\ell = e, \mu$), distributions of several kinematic variables, and recently the longitudinal tau polarization, $P_\tau^{D^*}$, in the D^* mode [8]. While the results on differential decay rates and $P_\tau^{D^*}$ are still statistically limited, the experimental values of $R(D^{(*)})$ already challenge the SM and some of its extensions. The current world averages of $R(D) = 0.407 \pm 0.039 \pm 0.024$ and $R(D^*) = 0.306 \pm 0.013 \pm 0.007$ [13] exceed the SM predictions $R(D) = 0.299 \pm 0.003$ [14], and $R(D^*) = 0.257 \pm 0.003$ [15] by 2.3 and 3.0 standard deviations (σ), respectively, and the combined results on $R(D^{(*)})$ deviate from the SM by about 3.8 σ . Interestingly, it is also difficult to accommodate the observed branching fractions within the two Higgs doublet models [16, 17], mainly due to the relatively large excess in the $B \rightarrow \bar{D}^*\tau^+\nu_\tau$ mode, which is expected to be less sensitive to the charged Higgs contributions than the $B \rightarrow \bar{D}\tau^+\nu_\tau$ channel. Further studies of kinematic distributions and angular observables in semitauonic B decays may provide new clues to unravel the $R(D^{(*)})$ puzzle. An interesting observable, not explored so far experimentally, is the D^* polarization. In the SM, the fraction of D^* longitudinal polarization, $F_L^{D^*}$, is expected to be around 0.45 [3, 18–21], and the most recent predictions are 0.441 ± 0.006 [20], and 0.457 ± 0.010 [21]. The value of $F_L^{D^*}$ can be significantly modified in the presence of NP contributions [3, 19–22]; in particular, the scalar and tensor operators may enhance and decrease $F_L^{D^*}$, respectively. In this paper, we present the first measurement of the D^* polarization in the $B^0 \rightarrow D^{*-}\tau^+\nu_\tau$ decay. We extract $F_L^{D^*}$ from the angular distribution in $D^{*-} \rightarrow \bar{D}^0\pi^-$ decay:

$$\frac{1}{\Gamma} \frac{d\Gamma}{d \cos \theta_{\text{hel}}} = \frac{3}{4} (2F_L^{D^*} \cos^2 \theta_{\text{hel}} + (1 - F_L^{D^*}) \sin^2 \theta_{\text{hel}}), \quad (1)$$

where θ_{hel} is the angle between \bar{D}^0 and the direction opposite to B^0 in the D^{*-} rest frame.

DETECTOR AND DATA SAMPLES

This analysis is based on the full $\Upsilon(4S)$ data sample containing $772 \times 10^6 \bar{B}B$ pairs recorded with the Belle detector at the asymmetric-beam-energy e^+e^- collider KEKB [23]. The Belle detector, described in detail elsewhere [24], is a large-solid-angle magnetic spectrometer that consists of a silicon vertex detector (SVD), a 50-layer central drift chamber (CDC), an array of aerogel threshold Cherenkov counters (ACC), a barrel-like arrangement of time-of-flight scintillation counters (TOF), and an electromagnetic calorimeter (ECL) comprised of CsI(Tl) crystals located inside a superconducting solenoid coil that provides

a 1.5 T magnetic field. An iron flux-return located outside of the coil is instrumented to detect K_L^0 mesons and to identify muons (KLM). Two inner detector configurations were used. A 2.0 cm radius beampipe and a 3-layer SVD was used for the first sample of 152×10^6 $B\bar{B}$ pairs, while a 1.5 cm radius beampipe, a 4-layer SVD and a small-cell inner drift chamber were used to record the remaining 620×10^6 $B\bar{B}$ pairs [25]. The analysis procedure is established using Monte Carlo (MC) samples. Particle decays are modeled by the EvtGen package [26], and followed by detector simulation performed with GEANT3 [27]. Radiative effects are modeled by PHOTOS [28]. Two large samples (100×10^6 events each) of $B^0 \rightarrow D^{*-} \tau^+ \nu_\tau$ decays are simulated within the SM using hadronic form factors based on the Isgur-Scora-Grinstein-Wise (ISGW) model [29] and on heavy quark effective theory (HQET) [3], respectively. To model the background, we use MC samples of continuum $q\bar{q}$ ($q = u, d, s, c$), and inclusive $B\bar{B}$ decays. The sizes of these samples are, respectively, six and ten times that of the collision data. Additionally, we use a sample of semileptonic B decays to orbitally-excited charmed mesons $B \rightarrow \bar{D}^{**} \ell^+ \nu_\ell$ (\bar{D}^{**} stands for \bar{D}_1 , \bar{D}_2^* , \bar{D}'_1 , and \bar{D}_0^*) generated with the ISGW model and decay kinematics corrected to match the Leibovich-Ligeti-Stewart-Wise model [30], that exceeds six times the data sample.

SIGNAL RECONSTRUCTION

The analysis adopts the approach of Refs. [4, 5]; signal decays (B_{sig}) are reconstructed first, and the accompanying B meson (B_{tag}) is reconstructed inclusively from all the particles that remain after selecting the B_{sig} candidate. We use the following secondary B_{sig} decays: $\tau^+ \rightarrow \ell^+ \nu_\ell \bar{\nu}_\tau$, $\pi^+ \bar{\nu}_\tau$, $D^{*-} \rightarrow \bar{D}^0 \pi^-$, $\bar{D}^0 \rightarrow K^+ \pi^-$, $K^+ \pi^- \pi^0$, $K^+ \pi^+ \pi^- \pi^-$ (denoted hereinafter as $K\pi$, $K\pi\pi^0$ and $K3\pi$, respectively). Primary charged tracks are required to have impact parameters consistent with an origin at the interaction point (IP), and to have momenta in the laboratory frame above 50 MeV [31]. K_S^0 mesons are reconstructed using pairs of charged tracks (treated as pions) satisfying the invariant mass requirement $482 \text{ MeV} < M_{\pi^+ \pi^-} < 514 \text{ MeV}$ with a vertex displacement from the IP consistent with the reconstructed momentum vector. Muons, electrons, charged pions, kaons and protons are identified using information from the particle identification subsystems. The momenta of particles identified as electrons are corrected for bremsstrahlung by adding photons within a 50 mrad cone along the lepton trajectory. The π^0 candidates are reconstructed from photon pairs having $118 \text{ MeV} < M_{\gamma\gamma} < 150 \text{ MeV}$. For candidates that share a common γ , we select the one with the smallest χ^2 value resulting from a π^0 mass-constrained fit. To reduce the combinatorial background, we require that the photons from the π^0 have energies greater than 50 MeV in the barrel part of the ECL and greater than 100 MeV in the end-caps. Photons that are not associated with a π^0 are accepted if their energy exceeds a polar-angle dependent threshold ranging from 100 MeV to 200 MeV.

The \bar{D}^0 candidates, formed in the above specified channels, are required to have masses in the range $-25(-30) \text{ MeV} < M_{\bar{D}^0} - m_{\bar{D}^0} < 25 \text{ MeV}$ for $\bar{D}^0 \rightarrow K\pi, K3\pi(K\pi\pi^0)$ around the nominal \bar{D}^0 mass, $m_{\bar{D}^0}$ [32], corresponding to a window of approximately $\pm 4.5(\pm 2.5)\sigma$. The D^{*-} candidates are reconstructed from $\bar{D}^0 \pi^-$ pairs; we require that the mass difference $\Delta M_{D^*} = M_{D^{*-}} - M_{\bar{D}^0}$ lie in the window $\pm 2.5 \text{ MeV} (\pm 3\sigma)$ around the nominal value of 145.43 MeV [32].

Signal candidates are selected by combining a D^{*-} meson with an oppositely charged electron, muon or pion. In the sub-channels with the $\tau^+ \rightarrow \pi^+ \bar{\nu}_\tau$ decay, the large combinatorial background is suppressed by requiring the pion energy to be more than 0.5 GeV. Particles

that are not assigned to B_{sig} are used to reconstruct the B_{tag} decay. The consistency of a B_{tag} candidate with a B -meson decay is checked using the beam-energy constrained mass and the energy difference variables in the $\Upsilon(4S)$ frame: $M_{\text{tag}} = \sqrt{(E_{\text{beam}}^2 - |\mathbf{p}_{\text{tag}}|^2)}$ and $\Delta E_{\text{tag}} = E_{\text{tag}} - E_{\text{beam}}$, where $\mathbf{p}_{\text{tag}} = \sum_i \mathbf{p}_i$, $E_{\text{tag}} = \sum_i E_i$, E_{beam} is the colliding-beam energy, and \mathbf{p}_i and E_i denote the 3-momentum vector and energy, respectively, of particle i . The summation is over all particles that are assigned to the B_{tag} candidate. We require that candidate events be in the range $M_{\text{tag}} > 5.2$ GeV and $-0.30 \text{ GeV} < \Delta E_{\text{tag}} < 0.05 \text{ GeV}$. The average number of candidates per event is about 1.03 for $(D^{*-}\ell^+)$ pairs and 1.08 for $(D^{*-}\pi^+)$ pairs. From multiple candidates, we select a $(D^{*-}d_\tau^+)$ pair (throughout the paper, d_τ stands for the charged τ daughter: e , μ , or π) with the best D^{*-} candidate, based on the value of ΔM_{D^*} . For the pairs sharing the same D^{*-} candidate, we perform a vertex fit to B_{tag} candidates, using all charged particles assigned to the tagging side, and select the one with the largest fit probability. Events with incorrectly or incompletely reconstructed B_{tag} are suppressed by imposing the following requirements: zero total event charge; no charged leptons in B_{tag} decay; zero net proton/antiproton number; E_{res} , the residual energy in the electromagnetic calorimeter (*i.e.*, the sum of energies of clusters that are not included in B_{sig} nor B_{tag}) less than 0.8 GeV, number of neutral particles on the tagging side $N_{\pi^0} + N_\gamma < 5$, and multiplicity of charged tracks $N_{\text{ch}} < 15$. For candidates with $d_\tau = \pi$, we require no K_L^0 candidate in the event. For further analysis, we accept events that satisfy requirements derived from the kinematics of signal decays: $q^2 \equiv M_W^2 = (p_{\text{sig}} - p_{D^{*-}})^2 > 4 \text{ GeV}^2$, ($p_{\text{sig}} = (E_{\text{beam}}, -\mathbf{p}_{\text{tag}})$), and for $(D^{*-}\pi^+)$ candidates, $M_W^2 > M_{\text{miss}}^2 + m_\tau^2$ (m_τ denotes the nominal mass of the τ lepton, and the missing mass squared $M_{\text{miss}}^2 = (p_{\text{sig}} - p_{D^{*-}} - p_{d_\tau^+})^2$ corresponds to the square of the effective mass of the neutrino system). With these requirements, the M_{tag} distribution of the signal peaks at the B^0 mass with more than 80% (60%) of the events being contained in the region $M_{\text{tag}} > 5.26$ GeV for $d_\tau = \ell(\pi)$.

BACKGROUND SUPPRESSION AND CALIBRATION

To suppress background, we exploit observables that are sensitive to multiple neutrinos in the final state: the visible energy E_{vis} , which is the sum of the energies of all particles in the event, and the fraction $X_{\text{miss}} = (E_{\text{miss}} - |\mathbf{p}_{D^{*-}} + \mathbf{p}_{d_\tau^+}|) / \sqrt{E_{\text{beam}}^2 - m_{B^0}^2}$, where $E_{\text{miss}} = E_{\text{beam}} - (E_{D^{*-}} + E_{d_\tau^+})$ and m_{B^0} is the nominal B^0 mass, that approximates missing mass and does not depend on the B_{tag} reconstruction [4]. X_{miss} falls in the range $[-1, 1]$ for events with zero missing mass (*e.g.*, with a single neutrino) but takes larger values if there are more undetected particles (*e.g.*, multiple neutrinos). The requirements $E_{\text{vis}} < 8.7$ (8.8) GeV, and $X_{\text{miss}} > 1.5$ (1.0) for $d_\tau = \ell(\pi)$ are chosen to maximize the statistical figure of merit $\text{FOM} = N_S / \sqrt{N_S + N_B}$ (N_S and N_B denote the expected signal and background yields in the window $M_{\text{tag}} > 5.26$ GeV), assuming SM value of $\mathcal{B}(B^0 \rightarrow D^{*-}\tau^+\nu_\tau) = 1.45\%$. The M_{tag} distributions are expected to be flat for most background components, while the distribution of the signal remains unchanged. Residual peaking background stems from semileptonic decays $B^0 \rightarrow D^{*-}\ell^+\nu_\ell$ and $B \rightarrow D^{*-}X\ell^+\nu_\ell$ (including $B \rightarrow \bar{D}^{**}\ell^+\nu_\ell$). The abundance of these and other background components is calibrated to data, separately for each signal decay chain. The MC samples are divided into the following categories: $B \rightarrow \bar{D}^*\ell^+\nu_\ell$, $B \rightarrow \bar{D}^{**}\ell^+\nu_\ell$, hadronic B decays, and $c\bar{c}$ and $u\bar{u} + d\bar{d} + s\bar{s}$ continuum. Hadronic B decays are further split into two subcategories: events with correctly assigned daughters to mother decays, and random combinatorial. The normalizations of these components are determined

by fitting the experimental distributions of M_{tag} , ΔE_{tag} , X_{miss} , E_{miss} , E_{vis} , E_{d^+} , M_W^2 , E_{res} , and R_2 , the last being the ratio of the second and zeroth Fox-Wolfram moments [33]. The region $M_{\text{tag}} > 5.26$ GeV and $X_{\text{miss}} > 0.75$ for leptonic τ decays, or $X_{\text{miss}} > 0.5$ for $\tau \rightarrow \pi\nu$, where we expect enhanced signal contribution, is excluded from the fit. In the $(D^{*-}\pi^+)$ pairs, a large part of the background comes from fake \bar{D}^0 candidates. This component is fixed from a comparison of the data and the MC data in the side-bands of the m_{D^0} distributions. Assuming the branching fraction $\mathcal{B}(B^0 \rightarrow D^{*-}\tau^+\nu_\tau) = 1.45\%$, we expect in the signal enhanced region $M_{\text{tag}} > 5.26$ GeV and in the range $-1 \leq \cos \theta_{\text{hel}} \leq 0$ around 170 (200) signal (background) events for $(D^{*-}\ell^+)$ pairs and 115 (290) events for $(D^{*-}\pi^+)$ pairs.¹ In the latter case, the signal yield includes also cross-feed events from other τ decays, mainly from $\tau^+ \rightarrow \rho^+\bar{\nu}_\tau$. For leptonic τ decays, the main background contribution ($\approx 35\%$) comes from semileptonic B decays to excited charmed resonances. Events with fake $\bar{D}^{(*)}$ candidates constitute around 45% of the $(D^{*-}\pi^+)$ background.

FITTING PROCEDURE

The $\cos \theta_{\text{hel}}$ distribution is measured by dividing the range $-1 \leq \cos \theta_{\text{hel}} \leq 0$ into three equidistant bins. Signal yield in the I -th bin of $\cos \theta_{\text{hel}}$ is extracted from an extended unbinned maximum likelihood fit to the M_{tag} distributions in that bin using the following likelihood function:

$$\mathcal{L}^I = e^{-[N_s^I + \sum_k (N_{pI}^k + N_{bI}^k)]} \prod_{i=1}^{N^I} [N_s^I \sum_k w_k P_s^k(x_i) + \sum_k (N_{pI}^k P_s^k(x_i) + N_{bI}^k P_{bI}^k(x_i))], \quad (2)$$

where x_i is the M_{tag} value of the i^{th} event, the index k runs over decay chains, and N^I is the total number of events in the I^{th} bin of $\cos \theta_{\text{hel}}$ in data. The probability density functions (PDF), P_s^k , that describe signal and peaking background are parameterized using the Crystal-Ball (CB) function [34]. Our MC studies show that for a given type of d_τ , the shape of the CB component does not depend on $\cos \theta_{\text{hel}}$ and is the same for all \bar{D}^0 decays. PDFs denoted P_{bI}^k describe combinatorial background, and are parameterized with an ARGUS-function (AR) [35]. All shape parameters of the PDFs are determined from fits to the MC samples and fixed in the fit to data. The coefficients w_k contain reconstruction efficiencies and partial decay rates of individual decay chains, and are calculated using signal MC. N_s^I , N_{bI}^k , and N_{pI}^k are the yields of signal, combinatorial background and peaking background in the I^{th} bin of $\cos \theta_{\text{hel}}$, respectively. N_s^I and N_{bI}^k are free parameters of the fit, while N_{pI}^k are fixed to the values obtained from fits to MC samples and scaled to the data integrated luminosity. The signal yields obtained in the bins of $\cos \theta_{\text{hel}}$ are reweighted with the following scale factors $s_1 = 0.98 \pm 0.01$ ($-1 \leq \cos \theta_{\text{hel}} < -0.67$), $s_2 = 0.96 \pm 0.01$ ($-0.67 \leq \cos \theta_{\text{hel}} < -0.33$), and $s_3 = 1.08 \pm 0.01$ ($-0.33 \leq \cos \theta_{\text{hel}} < 0$), in order to correct for small acceptance variations along $\cos \theta_{\text{hel}}$. The quoted errors arise from statistical uncertainties of the signal MC.

The D^{*-} polarization is measured by fitting the obtained $\cos \theta_{\text{hel}}$ distribution using Equation 1, with $F_L^{D^*}$ as the only free parameter. The procedure has been tested by fitting ensembles of simulated experiments varying $F_L^{D^*}$ in the range of $0 \leq F_L^{D^*} \leq 1$. These

¹ The region $\cos \theta_{\text{hel}} > 0$ is excluded from the analysis due to strong acceptance artifacts caused by the low D^{*-} reconstruction efficiency.

pseudo-experiments are generated using the shapes of the fitted PDFs for the signal and background components and with the number of events Poisson-distributed around the expected yields. The pull distributions of the extracted $F_L^{D^*}$ values are consistent with standard normal distributions in the entire range of $F_L^{D^*}$.

As a cross check, we apply our procedure to measure the D^* polarization in decays $B^0 \rightarrow D^{*-} e^+ \nu_e$, and obtain the result $F_L^{D^*}(B^0 \rightarrow D^{*-} e^+ \nu_e) = 0.56 \pm 0.02$, which agrees well with the value of 0.54 (0.53) predicted in the covariant quark model (heavy quark limit) [18].

RESULTS

Applying the procedure described above to data, we obtain the following yields of signal in the three bins of $\cos \theta_{\text{hel}}$: $N_s^1 = 151 \pm 21$ ($-1 \leq \cos \theta_{\text{hel}} < -0.67$), $N_s^2 = 125 \pm 19$ ($-0.67 \leq \cos \theta_{\text{hel}} < -0.33$), and $N_s^3 = 55 \pm 15$ ($-0.33 \leq \cos \theta_{\text{hel}} < 0$), where the uncertainties are statistical. The corresponding statistical significances are $\Sigma_1 = 8.8\sigma$, $\Sigma_2 = 7.8\sigma$, and $\Sigma_3 = 4.1\sigma$, respectively. The statistical significances are defined as $\Sigma_I = \sqrt{-2 \ln(\mathcal{L}_0^I / \mathcal{L}_{\text{max}}^I)}$, where $\mathcal{L}_{\text{max}}^I$ and \mathcal{L}_0^I denote the maximum likelihood value and the likelihood values for the zero signal hypothesis. Fit projections are shown in Figs. 1–3.

The signal yields N_s^I are weighted for acceptance corrections using the scale factors s_I . By fitting Eq. 1 to the obtained $\cos \theta_{\text{hel}}$ distribution, we measure $F_L^{D^*} = 0.60 \pm 0.08$ (statistical) with $\chi^2/ndf = 1.95/2$. The fit result is shown in Fig. 4.

Systematic uncertainties

The measurement of $F_L^{D^*}$ is not affected by absolute normalization of the signal yield. Therefore, uncertainties related to the number of $B\bar{B}$ pairs, B_{tag} reconstruction efficiency, and those coming from the limited accuracy of the partial branching fractions used in the analysis have no (or negligible) effect on the final result.

The dominant systematic uncertainties arise from the limited size of the MC sample and imperfect modelling of real processes. They are summarized in Table I and described below.

To evaluate the effect of statistical uncertainties of the MC-determined parameters that describe the shapes of the PDF, relative proportion of peaking background, scale factors of background components, and correction factors for the acceptance non-uniformities, the procedure of $F_L^{D^*}$ measurement is repeated by varying each parameter 1000 times at random, assuming Gaussian errors, and taking into account correlations among them. The standard deviation of the obtained $F_L^{D^*}$ distribution represents the corresponding systematic uncertainty.

In the second category, the poor knowledge of semileptonic B decays to excited charmed mesons, representing a large part of the peaking background, is an important source of systematic uncertainty. For $B \rightarrow \bar{D}^{**}\ell\nu$ modes, the branching fractions are varied for each D^{**} resonance within experimental uncertainties: $\pm 6\%(D_1)$, $\pm 10\%(D_2^*)$, $\pm 83\%(D'_1)$, and $\pm 100\%(D_0^*, D^{(*)}(2D))$ (assuming branching fractions of 0.5% for modes with radially excited states, $D^{(*)}(2S)$). Uncertainties related to the form factor parameterization are negligible. Uncertainty coming from $B \rightarrow \bar{D}^{**}\tau\nu$ decays, with the expected $\mathcal{B}(B \rightarrow \bar{D}^{**}\tau\nu) \approx 0.3\%$, is evaluated by changing their contribution by $\pm 100\%$ in the $B\bar{B}$ MC sample.

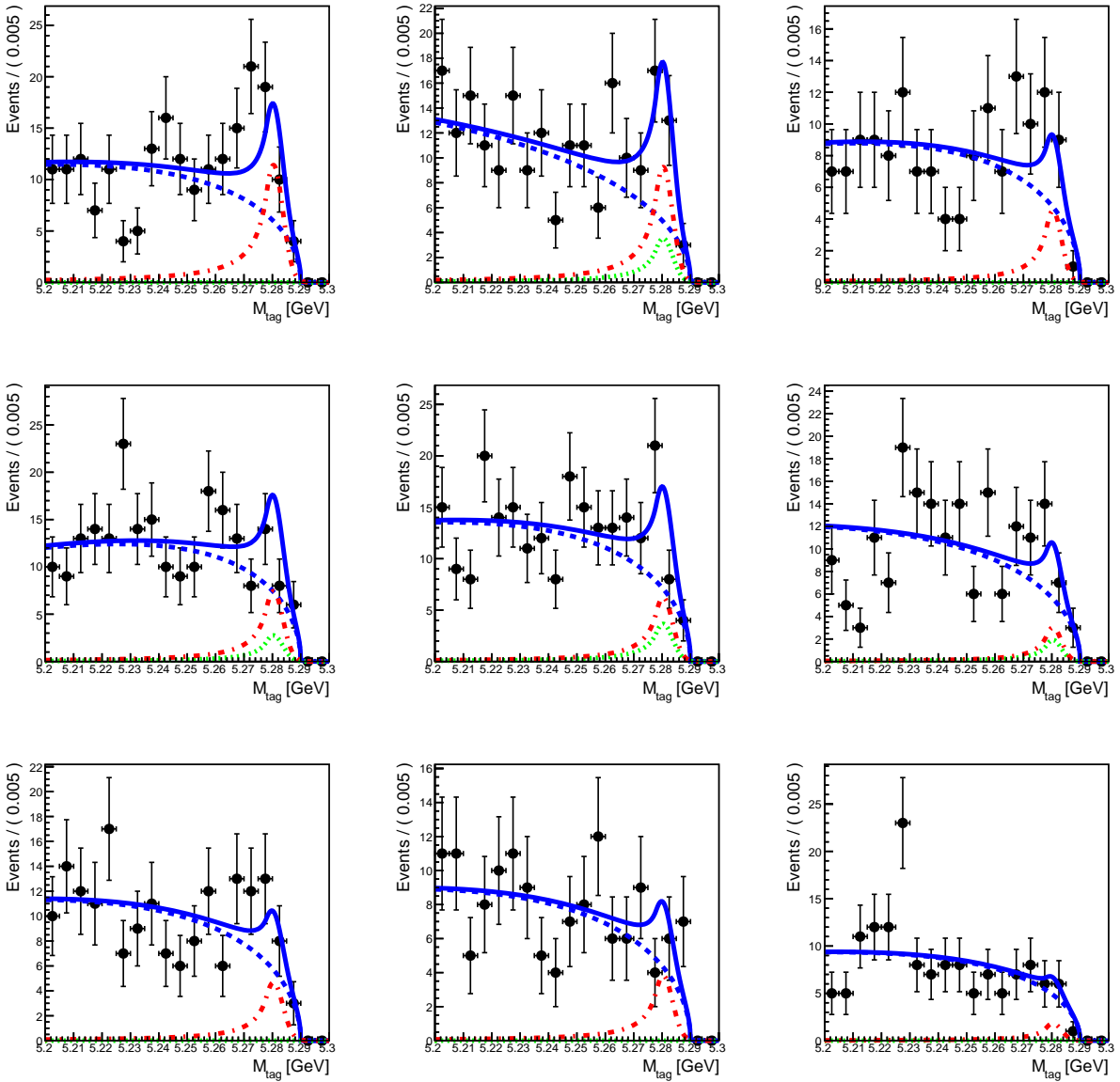


FIG. 1. Fit projections to M_{tag} distributions in three bins of $\cos \theta_{\text{hel}}$ for $\tau \rightarrow \pi \nu_\tau$ (sequential columns) and $D \rightarrow K\pi$ (top), $D \rightarrow K\pi\pi^0$ (middle), $D \rightarrow K3\pi$ (bottom). The solid lines show the result of the fit. Contributions of the signal, combinatorial and peaking backgrounds are represented by the red (dot-dashed), blue (dashed) and green (dotted) lines, respectively.

To estimate the uncertainties of combinatorial background from hadronic B decays, we vary within $\pm 50\%$ the relative fractions of 2-body, 3-body and n-body ($n > 3$) hadronic channels. Two-body decays of the type $B \rightarrow \bar{D}^* M$, where M denotes a meson with a mass $M_M > 2$ GeV, with correctly assigned daughters to B_{sig} and B_{tag} decays, represent the main peaking background in the $\tau \rightarrow \pi \nu_\tau$ mode. The systematic uncertainty coming from the composition of the M states (mainly the $c\bar{s}$ resonances) is evaluated by reweighting the q^2 spectrum by $\pm 100\%$ in two ranges of q^2 : $q^2 < 6.2$ GeV 2 and $q^2 > 6.2$ GeV 2 . (At $q^2 \approx 6.2$

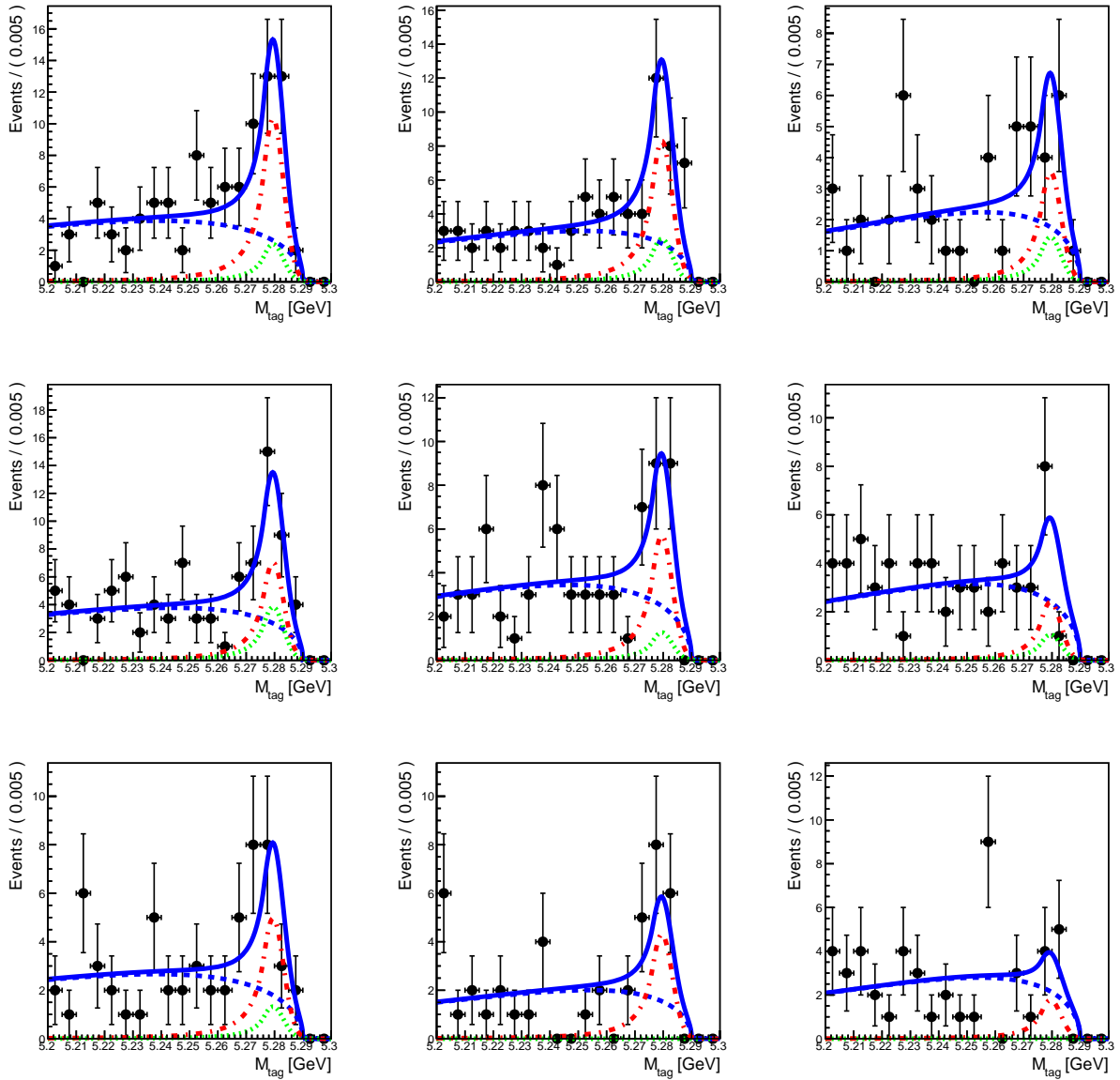


FIG. 2. Fit projections to M_{tag} distributions in three bins of $\cos \theta_{\text{hel}}$ for $\tau \rightarrow e\bar{\nu}_e\nu_\tau$ (sequential columns) and $D \rightarrow K\pi$ (top), $D \rightarrow K\pi\pi^0$ (middle), $D \rightarrow K3\pi$ (bottom). The solid lines show the result of the fit. Contributions of the signal, combinatorial and peaking backgrounds are represented by the red (dot-dashed), blue (dashed) and green (dotted) lines, respectively.

GeV² there is a sharp change in the $\cos \theta_{\text{hel}}$ distribution for this component.)

Uncertainties due to the form factor parameterization of signal decays are estimated by comparing the results obtained with the two versions of the signal MC, and found to be very small. Uncertainties related to the $\cos \theta_{\text{hel}}$ resolution and acceptance non-uniformities along $\cos \theta_{\text{hel}}$ depend on the actual value of the D^* polarization. To evaluate them, the simulated signal events are reweighted to obtain $\cos \theta_{\text{hel}}$ distributions that correspond to arbitrary D^* polarizations, and differences between the generated and measured values of

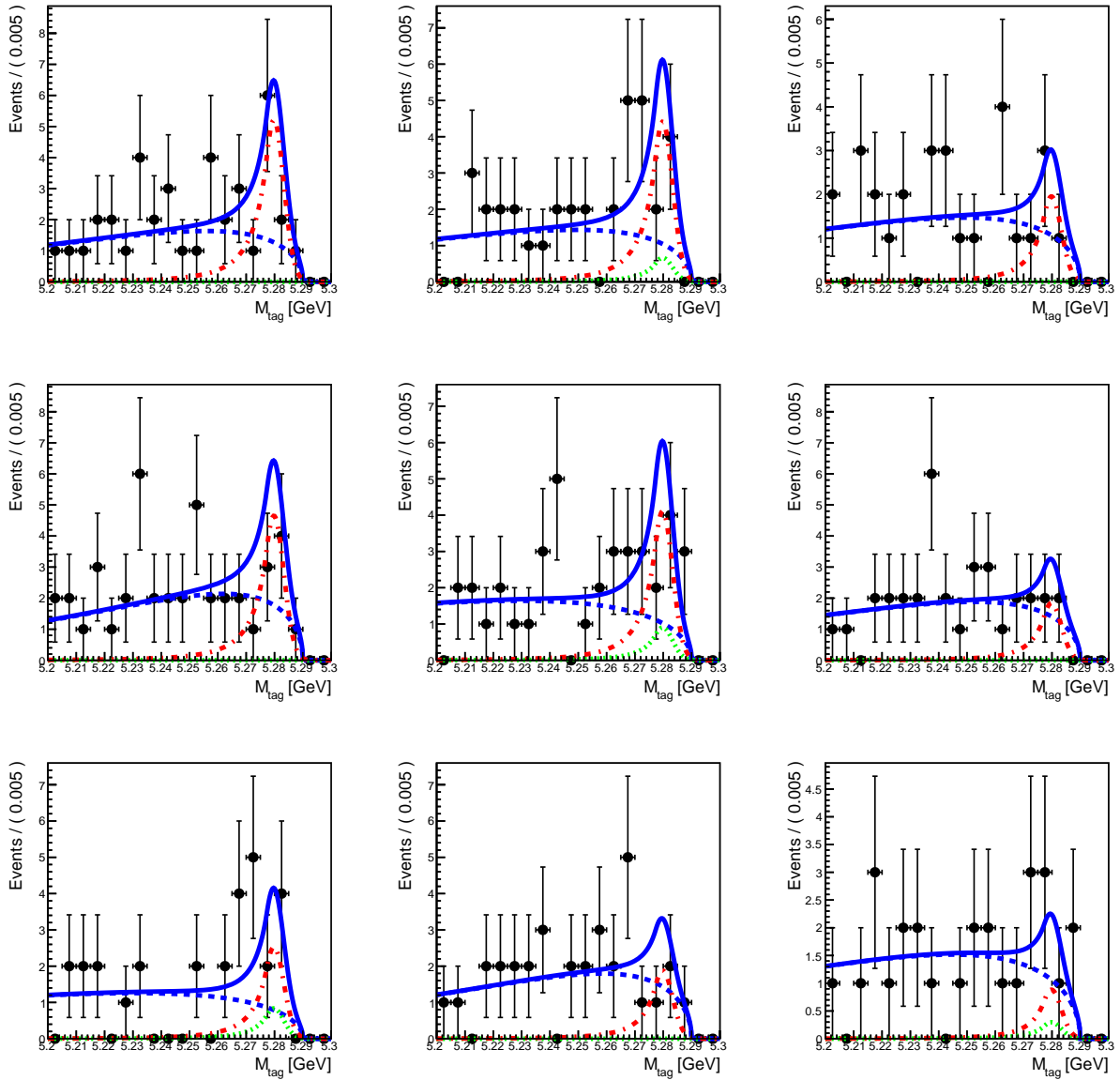


FIG. 3. Fit projections to M_{tag} distributions in three bins of $\cos \theta_{\text{hel}}$ for $\tau \rightarrow \mu \bar{\nu}_\mu \nu_\tau$ (sequential columns) and $D \rightarrow K\pi$ (top), $D \rightarrow K\pi\pi^0$ (middle), $D \rightarrow K3\pi$ (bottom). The solid lines show the result of the fit. Contributions of the signal, combinatorial and peaking backgrounds are represented by the red (dot-dashed), blue (dashed) and green (dotted) lines respectively.

$F_L^{D^*}$ are considered as systematic uncertainties. Uncertainties due to imperfect modeling of the $\cos \theta_{\text{hel}}$ resolution are within ± 0.003 in the full range of $F_L^{D^*}$ values. Variation of the $\cos \theta_{\text{hel}}$ distribution affects the correction factors s_I , resulting in the uncertainty of $^{+0.015}_{-0.005}$ for the measured value of $F_L^{D^*} = 0.60$.

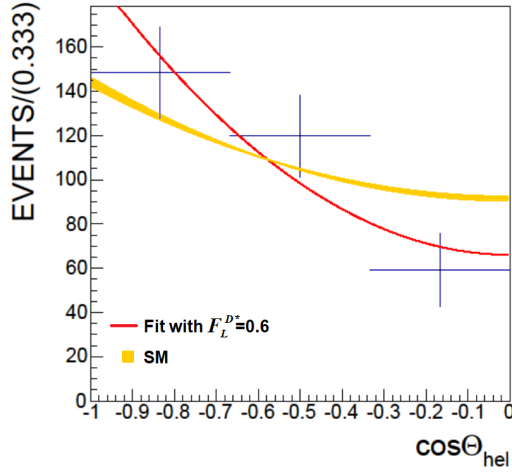


FIG. 4. The measured $\cos \theta_{\text{hel}}$ distribution in $B^0 \rightarrow D^{*-} \tau^+ \nu_\tau$ decays (data points with statistical errors); the fit result is overlaid (red line) with $F_L^{D^*} = 0.60$. The yellow band represents the SM prediction of Ref. [20].

TABLE I. Summary of systematic uncertainties

Source		$\Delta F_L^{D^*}$
Monte Carlo statistics	AR shape and peaking background	± 0.032
	CB shape	± 0.010
	Background scale factors	± 0.001
Background modeling	$B \rightarrow D^{**} \ell \nu$	± 0.003
	$B \rightarrow D^{**} \tau \nu$	± 0.011
	$B \rightarrow \text{hadrons}$	± 0.005
	$B \rightarrow \bar{D}^* M$	± 0.004
Signal modeling	Form factors	± 0.002
	$\cos \theta_{\text{hel}}$ resolution	± 0.003
	Acceptance non-uniformity	$+0.015$ -0.005
Total		$+0.039$ -0.037

CONCLUSIONS

We report the first measurement of the D^* polarization in semitauonic decay $B^0 \rightarrow D^{*-} \tau^+ \nu_\tau$. The result is based on a data sample of $772 \times 10^6 B\bar{B}$ pairs collected with the Belle detector. The fraction of D^{*-} longitudinal polarization, measured assuming SM dynamics, is found to be $F_L^{D^*} = 0.60 \pm 0.08(\text{stat}) \pm 0.04(\text{syst})$, and agrees within 1.6 (1.8) standard deviations with the SM predicted values $(F_L^{D^*})_{\text{SM}} = 0.457 \pm 0.010$ [21] (0.441 ± 0.006 [20]).

We thank the KEKB group for the excellent operation of the accelerator, the KEK cryogenics group for the efficient operation of the solenoid, and the KEK computer group and

the National Institute of Informatics for valuable computing and SINET3 network support. We acknowledge support from the Ministry of Education, Culture, Sports, Science, and Technology of Japan and the Japan Society for the Promotion of Science; the Australian Research Council and the Australian Department of Education, Science and Training; the National Natural Science Foundation of China under contract No. 10575109 and 10775142; the Department of Science and Technology of India; the BK21 program of the Ministry of Education of Korea, the CHEP SRC program and Basic Research program (grant No. R01-2005-000-10089-0) of the Korea Science and Engineering Foundation, and the Pure Basic Research Group program of the Korea Research Foundation; the Polish State Committee for Scientific Research; the Ministry of Education and Science of the Russian Federation and the Russian Federal Agency for Atomic Energy; the Slovenian Research Agency; the Swiss National Science Foundation; the National Science Council and the Ministry of Education of Taiwan; and the U.S. Department of Energy.

- [1] Throughout this paper, the inclusion of the charge-conjugate mode decay is always implied.
- [2] S. Fajfer, J. Kamenik, and I. Nisandzic, Phys. Rev. D **85**, 094025 (2012).
- [3] M. Tanaka and R. Watanabe, Phys. Rev. D **87**, 034028 (2013).
- [4] A. Matyja *et al.* (Belle Collaboration), Phys. Rev. Lett. **99**, 191807 (2007).
- [5] A. Bozek *et al.* (Belle Collaboration), Phys. Rev. D **82**, 072005 (2010).
- [6] M. Huschle *et al.* (Belle Collaboration), Phys. Rev. D **92**, 072014 (2015).
- [7] Y. Sato *et al.* (Belle Collaboration), Phys. Rev. D **94**, 072007 (2016).
- [8] S. Hirose *et al.* (Belle Collaboration), Phys. Rev. Lett. **118**, 211801 (2017), Phys. Rev. D **97**, 012004 (2018).
- [9] B. Aubert *et al.* (BaBar Collaboration), Phys. Rev. Lett. **100**, 021801 (2008).
- [10] J. P. Lees *et al.* (BaBar Collaboration), Phys. Rev. Lett. **109**, 101802 (2012), Phys. Rev.D **88**, 072012 (2013).
- [11] R. Aaij *et al.* (LHCb Collaboration), Phys. Rev. Lett. **115**, 111803 (2015).
- [12] R. Aaij *et al.* (LHCb Collaboration), Phys. Rev. Lett. **120**, 171802 (2018).
- [13] Heavy Flavor Averaging Group, <https://hflav.web.cern.ch>.
- [14] P. Gambino and D. Bigi, Phys. Rev. D **94**, 094008 (2016).
- [15] F. Bernlochner, Z. Ligeti, M. Papucci, and D. Robinson, Phys. Rev. D **95**, 115008 (2017), Erratum: Phys. Rev. D **97**, 059902 (2018).
- [16] A. Celis, M. Jung, X.-Q. Li, and A. Pich, JHEP **01**, 054 (2013).
- [17] S. Iguro and K. Tobe, Nucl. Phys. B **925**, 560 (2017).
- [18] M. A. Ivanov, J. G. Körner, and C. T. Tran, Phys. Rev. D **92**, 114022 (2015).
- [19] A. K. Alok, D. Kumar, S. Kumbahar, and S. U. Sankar, Phys. Rev. D **95**, 115038 (2017).
- [20] Z.-R. Huang, Y. Li, M. Ali Paracha, and C. Wang, Phys. Rev. D **98**, 095018 (2018).
- [21] S. Bhattacharya, S. Nandi, and S. K. Patra, arXiv:1805.08222 [hep-ph].
- [22] M. A. Ivanov, J. G. Körner, and C. T. Tran, Phys. Rev. D **94**, 094028 (2016).
- [23] S. Kurokawa and E. Kikutani, Nucl. Instr. Methods Phys. Res., Sect. A **499**, 1 (2003), and other papers included in this volume.
- [24] A. Abashian *et al.* (Belle Collaboration), Nucl. Instr. Methods Phys. Res., Sect. A **479**, 117 (2002); also see detector section in J. Brodzicka *et al.*, Prog. Theor. Exp. Phys. **2012**, 04D001 (2012).

- [25] Z. Natkaniec *et al.* (Belle SVD2 Group), Nucl. Instr. Methods Phys. Res., Sect. A **560**, 1 (2006).
- [26] D. J. Lange, Nucl. Instr. Methods Phys. Res., Sect. A **462**, 152 (2001).
- [27] R. Brun *et al.*, GEANT 3.21, CERN Report DD/EE/84-1, 1984.
- [28] E. Barberio and Z. Wąs, Comput. Phys. Commun. **79**, 291 (1994).
- [29] D. Scora and N. Isgur, Phys. Rev. D **52**, 2783 (1995).
- [30] A. K. Leibovich, Z. Ligeti, I. W. Stewart, and M. B. Wise, Phys. Rev. D **57**, 308 (1998).
- [31] Natural units system with $\hbar = c = 1$ is used.
- [32] C. Patrignani *et al.* (Particle Data Group), Chin. Phys. C **40**, 100001 (2016).
- [33] G. C. Fox and S. Wolfram, Phys. Rev. Lett. **41**, 1581 (1978).
- [34] T. Skwarnicki, Ph.D. Thesis, Institute of Nuclear Physics, Krakow 1986; DESY Internal Report, DESY F31-86-02 (1986)
- [35] H. Albrecht *et al.* (ARGUS Collaboration), Phys. Lett. B **241**, 278 (1990).